Form of Al–Ti Oxide Produced by Al–Ti Deoxidation Reaction at 1873 and 1473 K

Hiroyuki Matsuura
Lecturer
Department of Advanced Materials Science,
Graduate School of Frontier Sciences,
The University of Tokyo

1. Introduction

Titanium-alloyed steels have been widely used for various products such as automobile sheets, heavy plates, or stainless steels, because titanium has great advantages not only in cost effectiveness but also in improvements of physical and chemical properties of steels, such as formability, non-ageing property, prevention of austenite grain growth, or promotion of fine ferrite microstructure formation. It is well known that titanium forms various non-metallic inclusions, *e.g.* oxide, nitride, carbide, or sulfide; especially titanium oxide exists in several forms such as Ti_2O_3, Ti_3O_5, TiO and so on, depending on steel compositions.

Since titanium has a strong affinity with oxygen, it is normally alloyed after deoxidation process. Aluminum is one of common strong deoxidizer. Titanium is much expensive raw material compared to aluminum, and therefore the combined process of deoxidation by aluminum and alloying by titanium is popular. The Al–Ti deoxidation process is one of the common processes for secondary refining. Thermodynamics for Al deoxidation or Ti deoxidation reaction have been studied well, while the complex deoxidation by Al and Ti addition has not been comprehensively understood. Ruby-Meyer *et al.*[1] have estimated the stable oxide phases equilibrated with Fe–Al–Ti melts by employing the multiphase equilibrium code CEQCSI based on the IRSID slag model[2] at 1793 K. The calculated stable phase diagram indicates the formation of Al_2O_3, Ti_2O_3, Al_2TiO_5 or TiO_x–Al_2O_3 liquid oxide. On the contrary, Jung *et al.*[3] have employed FACT databases and FactSage software, and calculated the similar phase diagram of oxides for the Fe–Al–Ti–O system at 1873 K. They have reported the stable region of a Ti_3O_5 solid phase which have not existed in the reported diagram by Ruby-Meyer *et al.*,[1] while they have not found a liquid phase. Later, they have revised the previous phase diagram in which stable regions of Al_2O_3, Ti_2O_3, Ti_3O_5 and liquid oxide equilibrating with metal are shown.[4] Kim *et al.* also reported the phase stability diagram of oxides equilibrating with Fe–Al–Ti melt at 1873 K. The stable regions for Al_2O_3, Ti_2O_3 and Ti_3O_5 were shown, while those for other oxides and liquid oxides were not observed.[5] As a conclusion, the chemical stability of Al–Ti–O oxides equilibrating with metal is still open for discussion.

The stability of non-metallic inclusions containing titanium in solid steel would be more complex due to the formation of not only oxide but also nitride, carbide, sulfide and

so on, which are normally not found at secondary refining temperatures. The behavior of non-metallic inclusions in solid state steel is quite important to understand the relationship between microstructure of steel and mechanical properties, and thus to maximally bring out such properties for best performance. Nevertheless, even the stability of oxides containing aluminum and/or titanium in solid steel at heat treatment temperatures has not been clarified.

In the present study, firstly the stable region of Al_2TiO_5 which has not been experimentally measured among various oxides produced by Al–Ti deoxidation, was measured by chemical equilibration technique at 1873 K. Secondly, the evolution and modification of oxide inclusions in Fe–Al–Ti steels were investigated and the change in inclusion compositions, morphologies and size with heating time was discussed.[6)]

2. Experimental

2.1. Equilibrium between Al_2TiO_5 and Fe–Al–Ti melt

Firstly Fe–Al–Ti metals (Al: 0.0142 to 0.1088 mass%, Ti: 0.0380 to 0.3875 mass%) were prepared by following procedure. About 150 g of solid electrolytic iron were put in a porous MgO crucible (OD 38 mm, ID 26 mm and height 123 mm) and then the crucible was put inside a quartz reaction tube (OD 50 mm, ID 46 mm and length 360 mm). After the atmosphere inside the reaction tube was changed to Ar gas (purity 99.9 %, flow rate 400 cm^3/min), the prepared electrolytic iron was heated and melted by an induction furnace at 1873 K for 1 h. After that Al (purity 99.9 %) and Ti (purity 99.9 %) were added in sequence with interval of 2 min. Finally the crucible was taken out from the reaction tube at 10 min after titanium addition, and quenched by water.

Al_2TiO_5 powder was produced by mixing reagent grade Al_2O_3 and TiO_2 powders in equimolar amounts and sintering about 20 g of the mixture at 1823 K for 24 h inside an Al_2O_3 crucible (OD 38 mm, ID 34 mm and height 45 mm). Obtained powder was compacted in a tablet shape of 18 mm diameter and 1 mm thickness and sintered at 1823 K for 24 h in an Al_2O_3 crucible to prepare the Al_2TiO_5 pellet.

Figure 1 shows the schematic diagram of equilibrium experimental apparatus. About 30 g of Fe–Al–Ti sample and 1 g of Al_2TiO_5 pellet were put in an Al_2O_3 crucible (OD 38 mm, ID 34 mm and height 45 mm). The crucible was suspended at the top of an Al_2O_3 reaction tube (OD60 mm, ID 52 mm, length 1000 mm) by winding with tungsten wire. The reaction tube atmosphere was changed to Ar gas and thus Ar–3%H_2 gas was introduced by 200 cm^3/min. Then, the crucible was moved down to the hot zone of the furnace. The crucible was quickly pulled up after 3 h and Ar gas was blown for quenching.

One gram of specimen was machined from each Fe–Al–Ti sample and dissolved into mixed acid (HCl : HNO_3 : Water = 1 : 2 : 5) and Al and Ti contents of solution were analyzed by ICP–OES (SII SPS7800) after filtration. Total oxygen content was analyzed by combustion – infrared absorption method (LECO TC600). X-ray diffraction pattern of

oxide pellet before and after experiment was measured by powder XRD equipment (RIGAKU RINT–2500V).

Metal–oxide pellet interfaces of some specimens were observed and analyzed by SEM–EDS. The specimen was mounted by polyester resin and polished by SiC papers and diamond suspensions up to 0.25 μm. Contents of Al, Fe, Mg and Ti in inclusions observed at the polished surface were determined by EDS (JEOL EX–54175JMU).

2.2. Observation of inclusions in metal deoxidized by Al–Ti

Three kinds of Fe–Al–Ti specimens (hereafter, named as 2–A, 2–B, and 2–C) were prepared. About 200 g of electrolytic iron was put in an MgO crucible (OD 38 mm, ID 26 mm, height 123 mm) and the crucible was put in a quartz tube (OD 50 mm, ID 46 mm, length 360 mm). After the atmosphere of the reaction tube was replaced to Ar gas (purity 99.9 %, flow rate 400 cm^3/min), the sample was melted in an induction furnace at 1873 K for 1 h, and then Al (purity 99.9 %) followed by Ti (purity 99.9 %) were added in sequence with interval of 2 min to specimens 2–A and 2–C, or only Ti was added to specimen 2–B. The melt was further kept for 10 min and then the crucible was taken out from the reaction tube and quenched by immersing a crucible into water. The same methods as 2.1. for analyses of Al, Ti and total O contents were employed.

A piece of sample (25 mm diameter, thickness 10 mm) was machined from each sample and hanged in the reaction tube of an electric furnace by steel wire. Then, samples were heated at 1473 K for 1 to 3 hours after the atmosphere was replaced by Ar gas (purity 99.9 %, flow rate 350 cm^3/min). After prescribed heating time, the sample was quickly taken out of the reaction tube and quenched by immersing into water.

The same procedures as 2.1. for sample preparation were applied to observe inclusions in as-cast and heated samples. Inclusions were characterized through observations by SEM (JEOL JSM–6060LV) and composition analyses by EDS (JEOL EX–54175JMU). Compositions of Al, Fe, Mg and Ti of inclusions were determined.

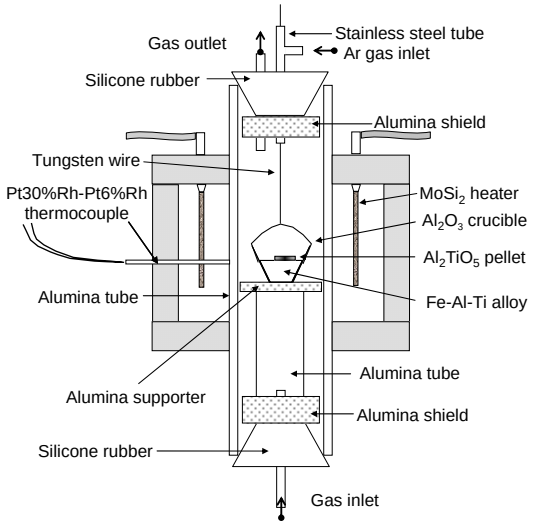

Figure 1　Schematic diagram of apparatus for equilibrium experiment.

3. Results and Discussion

3.1. Equilibrium between Al_2TiO_5 and Fe–Al–Ti melt

Table 1 shows the compositions of specimens after equilibrium experiments. Oxide pellets after experiments could be easily separated from metals after all experiments. However, it was expected from the position and shape of samples that oxide pellet and metal contacted well each other at 1873 K. In addition, since Al_2O_3 crucibles were used, molten metal was doubly saturated by Al_2TiO_5 and Al_2O_3. The shape of oxide pellet was the same as the green pellet and the formation of liquid oxide phase was not confirmed by visual observation.

The dissolution reactions of Al_2O_3 and Al_2TiO_5 into molten iron are expressed as Reactions (1) and (2). Interaction parameters applied for the calculation of Gibbs free energy changes from present results are shown in **Table 2**.[7–9)]

$$Al_2O_3\ (s) = 2\ \underline{Al}\ (mass\%) + 3\ \underline{O}\ (mass\%) \quad (1)$$

$$Al_2TiO_5\ (s) = 2\ \underline{Al}\ (mass\%) + \underline{Ti}\ (mass\%) + 5\ \underline{O}\ (mass\%) \quad (2)$$

Table 1 Results of equilibrium experiments.

Exp. No.	Compositions of metal (ppm)			Equilibrium constant (-)		ΔG° of dissolution (J/mol)	
	Sol. Al	Sol. Ti	T. O	Al_2O_3	Al_2TiO_5	Al_2O_3	Al_2TiO_5
1–1	16.3	342.4	50.6	2.98×10^{-13}	2.42×10^{-19}	449000	667000
1–2	0.74	1.5	249	6.5×10^{-14}	5.6×10^{-21}	470000	730000
1–3	0.94	5.1	145	2.3×10^{-14}	2.4×10^{-21}	490000	740000
1–4	0.66	1.2	203	3.0×10^{-14}	1.4×10^{-21}	490000	750000
1–5	0.67	1.3	272	6.8×10^{-14}	6.0×10^{-21}	470000	730000
1–6	2.2	10.2	82.6	2.5×10^{-14}	1.7×10^{-21}	490000	740000
1–7	105.8	2051	60.2	1.31×10^{-11}	6.70×10^{-17}	390000	580000
1–8	48.2	878.7	46.7	1.77×10^{-12}	2.86×10^{-18}	421000	629000
1–9	17.4	286.7	54.6	4.30×10^{-13}	3.43×10^{-19}	443000	662000
1–10	19.9	359.5	38.6	1.98×10^{-13}	9.85×10^{-20}	455000	682000
1–11	84.3	1836	47.3	4.37×10^{-12}	1.29×10^{-17}	407000	606000

Table 2 Interaction parameters.

e_i^j (j→)	Al	Ti	O
Al	0.0430[7)]	0.0040[9)]	−1.98[7)]
Ti	0.0037[9)]	0.049[8)]	−1.03[8)]
O	−1.17[7)]	−0.340[8)]	−0.17[7)]

Gibbs free energy changes of Reactions (1) and (2) calculated from experimental results are shown in Table 1. Average values of Gibbs free energy changes of the dissolution reaction of Al_2O_3 or Al_2TiO_5 into molten iron at 1873 K were determined as follows.

$$Al_2O_3\ (s) = 2\ \underline{Al}\ (mass\%) + 3\ \underline{O}\ (mass\%) \quad \Delta G^\circ = 450000\ J/mol \quad (1873\ K)$$

$$Al_2TiO_5\ (s) = 2\ \underline{Al}\ (mass\%) + \underline{Ti}\ (mass\%) + 5\ \underline{O}\ (mass\%)$$
$$\Delta G^\circ = 680000\ J/mol \quad (1873\ K)$$

Gibbs free energy change for Al_2O_3 dissolution reaction obtained from present study is almost the same as that reported by Itoh *et al.*,[7] 450600 J/mol.

The Al–Ti oxide stability diagram equilibrated with Fe–Al–Ti melt at 1873 K was calculated by using obtained Gibbs free energy changes for the dissolution reactions of Al_2O_3 and Al_2TiO_5 into molten iron, and reported equilibrium constants for the dissolution reactions of Ti_2O_3 and Ti_3O_5 expressed as Eqs. (3) and (4).[8] **Figure 2** shows the calculated stability diagram with present experimental results. In the present study, oxygen content of metal may be overestimated since total oxygen content in metal samples was analyzed by combustion method. Indeed, oxygen content of metal is larger than estimated by calculation.

$$Ti_2O_3\ (s) = 2\ \underline{Ti}\ (mass\%) + 3\ \underline{O}\ (mass\%) \quad \log K_{Ti_2O_3} = -9.986 \quad (1873\ K) \quad (3)$$
$$Ti_3O_5\ (s) = 3\ \underline{Ti}\ (mass\%) + 5\ \underline{O}\ (mass\%) \quad \log K_{Ti_3O_5} = -16.50 \quad (1873\ K) \quad (4)$$

Figure 3 shows the XRD patterns of an oxide pellet before and after an experiment. Only peaks corresponding to Al_2TiO_5 phase were observed in the case of oxide pellet before experiment, while both peaks corresponding to Al_2TiO_5 and Al_2O_3 phases were observed from the pellet after experiment. Therefore, the oxide pellet after experiment is the mixture of Al_2TiO_5 and Al_2O_3.

Compositions of oxides at the interface between metal and oxide pellet in some specimens were measured. **Figure 4** shows the typical interface of metal–oxide pellet. Light and dark gray regions were observed inside oxide pellet. Measured compositions of each phase were shown as the Fe–Al–Ti ternary system in the figure, in which light gray region is TiO_x phase containing approximately 10 mol%Al while dark gray region was Al_2O_3 phase containing about 3 mol%Ti. **Figure 5** shows the measured compositions of oxide phases observed at the metal–oxide pellet interfaces as the Al–Ti binary system. Initial Al_2TiO_5 phase (Ti content as the Al–Ti binary system is 33.3 mol%) was not observed at the metal–oxide pellet interface, while Al_2O_3 phase containing TiO_x and TiO_x phase containing Al_2O_3 were observed. These different oxide phases were also confirmed from SEM images.

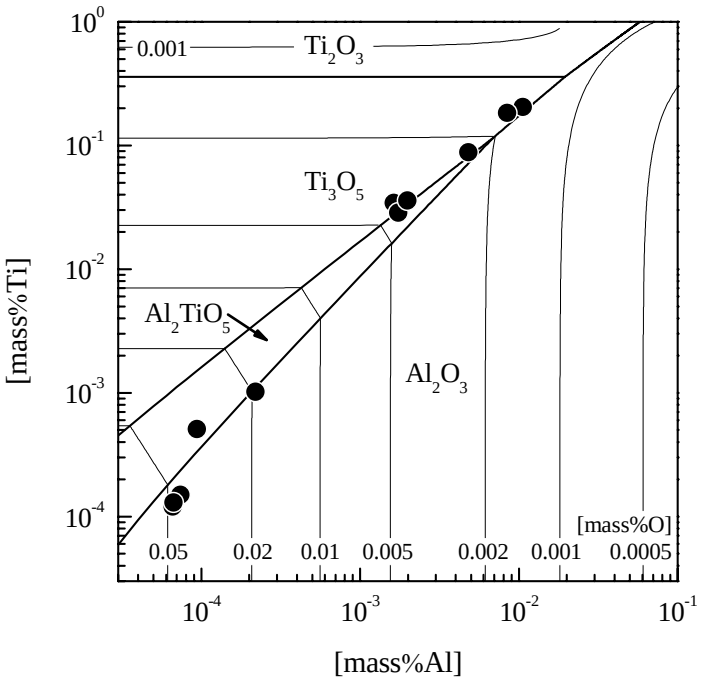

Figure 2　Compositions of metals after equilibrium on the calculated stable oxide phase diagram for the Fe–Al–Ti–O system equilibrated with molten Fe–Al–Ti at 1873 K.

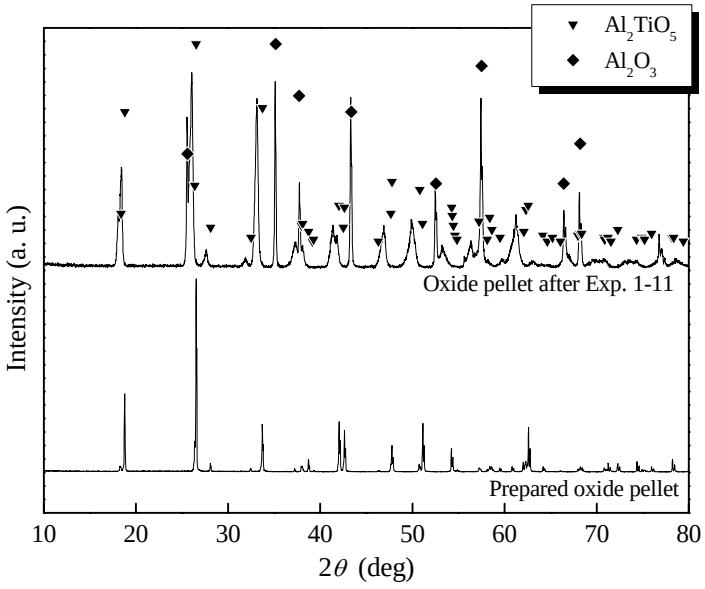

Figure 3　XRD patterns of oxide pellets before and after equilibrium experiment.

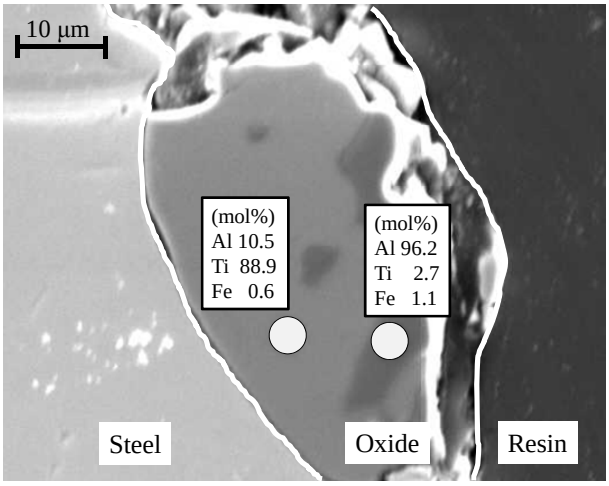

Figure 4　SEM image at the interface between metal and oxide phases, and compositions analyzed by EDS. (Exp. 1–11)

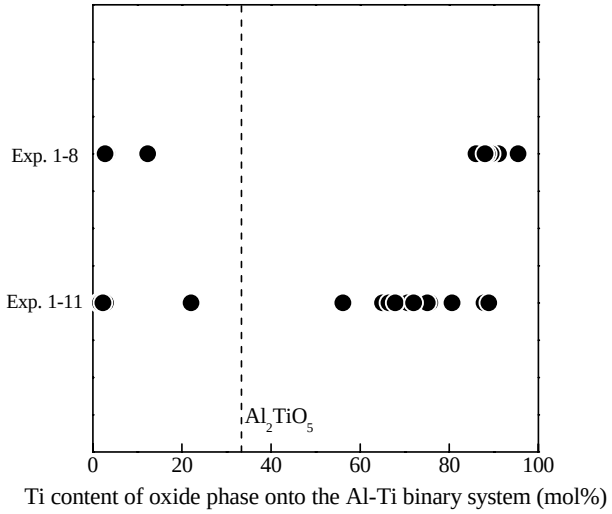

Figure 5　Compositions of oxide phase analyzed by EDS.

Oxide inclusions dispersed in some metals after experiments were analyzed to measure the compositions of oxide phases which could be equilibrated with metal sufficiently without any effect from gas phase. **Figure 6** shows the example of measured inclusions compositions onto the Al–Ti–Fe ternary system. Inclusion compositions were plotted on the line from the Fe corner because Fe contents of inclusions were overestimated due to the X-ray signal from Fe matrix during EDS analysis of fine inclusions, and thus precise analysis of Fe content of inclusions was hard. Therefore, measured inclusion compositions were converted to the Al–Ti binary system by removing Fe content for the sake of convenience. **Figure 7** shows the inclusion compositions converted to the Al–Ti binary system. Similar to the case of oxides at the metal – oxide pellet interfaces, Al_2TiO_5 oxide was not observed but Al_2O_3 phase containing TiO_x and TiO_x phase containing Al_2O_3 were found.

As a result, compositions of inclusions could not be estimated from the stability

diagram for the Al–Ti oxides equilibrated with the Fe–Al–Ti melts at 1873 K shown in Fig. 2. It was concluded that the further investigations are required to clarify the stable phases for the Al_2O_3–TiO_x oxide system.

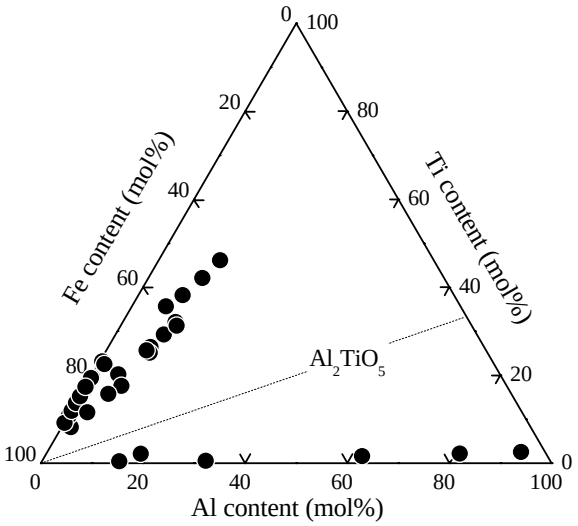

Figure 6 Projection of compositions of oxide inclusions on the Al–Ti–Fe ternary system. (Exp. 1–10)

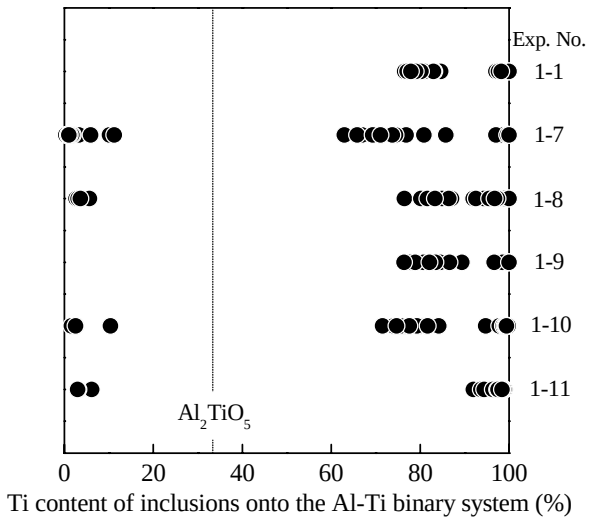

Figure 7 Compositions of oxide inclusions analyzed by EDS.

3.2. Observation of inclusions in metal deoxidized by Al–Ti

Compositions of prepared specimens are summarized in **Table 3**. According to the stability diagram shown in Fig. 2, compositions of specimens 2–A, 2–B and 2–C are located in the Al_2O_3 stable region, the Ti_3O_5 stable region, and at the boundary between Al_2O_3, Al_2TiO_5, Ti_2O_3 and Ti_3O_5 stable regions, respectively. Mg content in all inclusions of all specimens was lower than 1 mass%, and therefore the observed inclusions were considered as the Al_2O_3–FeO–TiO_x system.

Table 3 Compositions of specimens.

Exp. No.	Compositions of metal (mass%)		
	Sol. Al	Sol. Ti	T. O
2–A	0.0341	0.0444	0.0060
2–B	–	0.028	0.0007
2–C	0.0162	0.29	0.0035

(1) Specimen 2–A (Al: 0.0341 mass%, Ti: 0.0444 mass%)

Typical SEM images of inclusions in as-cast, and heated samples are shown in **Fig. 8**. The shape of inclusions in an as-cast sample was mainly spherical and it did not change clearly by heating at 1473 K.

Compositions of inclusions are represented on the Al–Fe–Ti ternary system as shown in **Fig. 9**. Most of inclusions observed in an as-cast sample had the composition of almost pure Al_2O_3 and Ti content in inclusions was less than 4 mol%. Although Fe content was observed up to 25 mol%, Fe content of smaller inclusions tend to increase due to the X-ray signal from Fe matrix. Therefore, the inclusion composition was concluded as almost pure Al_2O_3 containing small content of TiO_x.

The inclusion compositions changed from Al_2O_3 to Al–Fe–O, or Al–Ti–Fe–O system by heating at 1473 K, which were not observed in an as-cast sample. After 60 min, three types of inclusions were observed, namely Al_2O_3, Al–Fe–O, and Al–Ti–Fe–O inclusions. Most Al–Fe–O inclusions contained from 30 to 40 mol% Fe as the Al–Fe binary system. The composition of Al–Ti–Fe–O inclusions as the Al–Fe–Ti ternary system was in the range between 35 and 75 mol%Fe, and 5 and 20 mol%Ti.

After heating for 180 min at 1473 K, Al_2O_3 inclusion was no longer observed and only Al–Fe–O or Al–Fe–Ti–O inclusions were observed. Composition of Al–Fe–O inclusions dispersed widely and the Fe content as the Al–Fe binary system was between 30 and 75 mol%. The Al–Ti–Fe–O inclusions contained from 10 to 20 mol%Al, from 60 to 80 mol%Fe, and from 10 to 20 mol%Ti as the Al–Fe–Ti ternary system. Number of inclusions with large Fe content increased with increasing heating time. From these results, Al_2O_3 inclusions changed to Al–Fe–Ti–O inclusions by heating at 1473 K.

Figure 10 shows the size distribution of inclusions. The size distribution of inclusions was not affected clearly by heating although composition changed significantly.

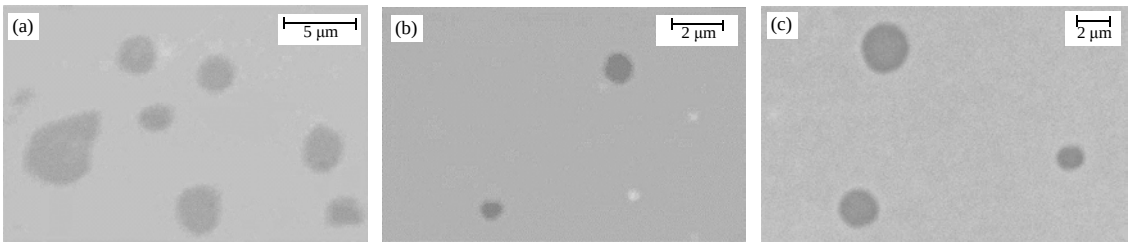

Figure 8 SEM images of typical inclusion observed in Specimen 2–A; (a) as cast, (b) after 60 min heating at 1473 K, and (c) after 180 min heating at 1473 K.

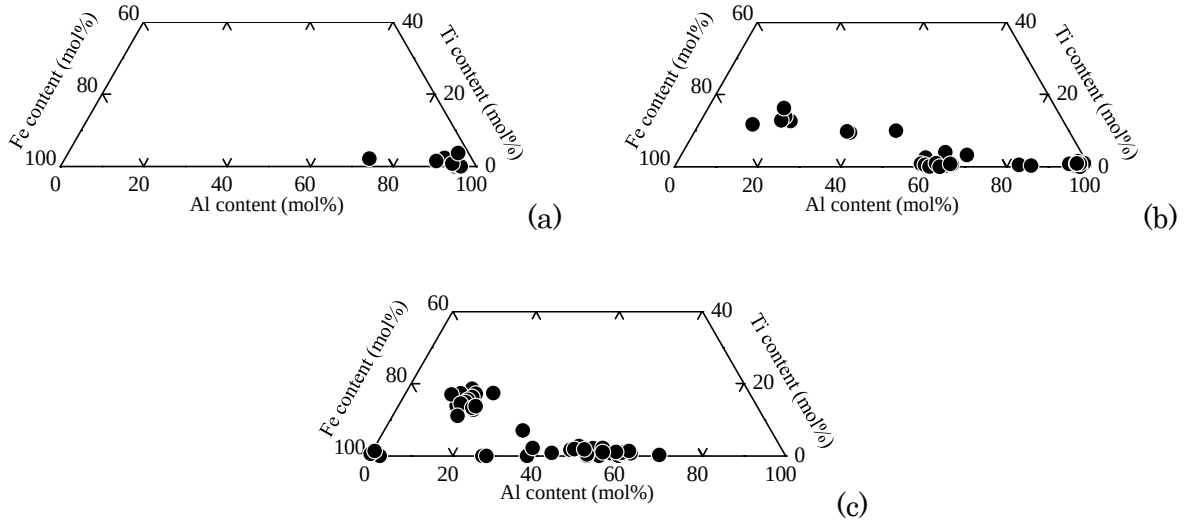

Figure 9　Composition of inclusions in Specimen 2–A; (a) as cast, (b) after 60 min heating at 1473 K, and (c) after 180 min heating at 1473 K.

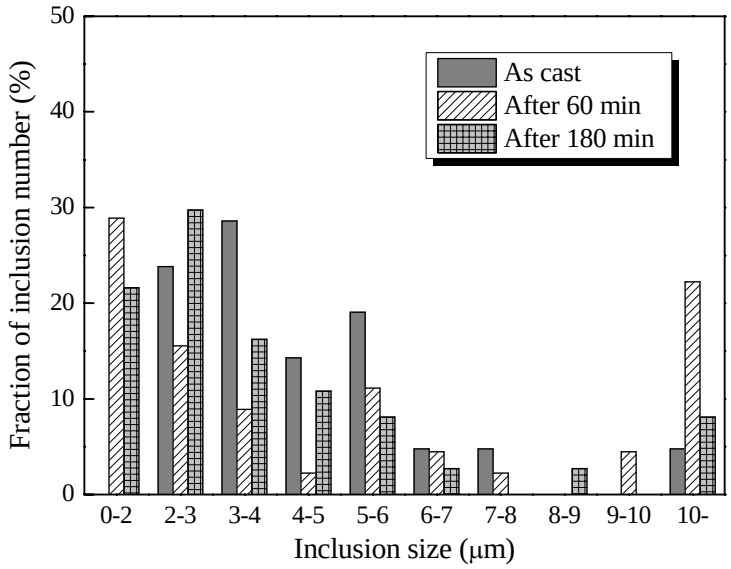

Figure 10　Size distribution of inclusions in Specimen 2–A; (a) as cast, (b) after 60 min heating at 1473 K, and (c) after 180 min heating at 1473 K.

(2) Specimen 2–B (Ti: 0.028 mass%)

Figure 11 shows the typical inclusion shapes in Specimen 2–B. Inclusions in an as-cast sample had very irregular shape, while mainly spherical shape inclusions were observed in samples after heating at 1473 K. The size of inclusions became smaller with heating time as explained in detail below.

Figure 12 shows the compositions of inclusions observed in Specimen 2–B. In an as-cast sample, TiO_x inclusions with small Fe content were mainly detected. On the contrary, Ti–Fe–O inclusions were observed in samples heated at 1473 K. In the sample heated at

1473 K for 60 min, Fe content as the Fe–Ti binary system varied from 50 to 100 mol% and the average composition was 75 mol%Fe–25 mol%Ti. Composition of inclusions in a sample heated for 180 min clearly showed the change in composition from TiO_x to 75 mol%Fe–25 mol%Ti as the Fe–Ti binary system.

Figure 13 shows the size distribution of inclusions. Inclusion size clearly became smaller with heating samples at 1473 K. In an as-cast sample, inclusion size dispersed widely from less than 1 to over 10 μm, while many fine inclusions were found in samples heated at 1473 K. More than half of observed inclusions in the heated sample for 180 min were in the size range between 2 and 3 μm.

From compositional and size change of inclusions during heating at 1473 K, it is considered that the dissolution of TiO_x inclusions into the metallic phase and the nucleation of smaller Fe–Ti–O inclusions occurred simultaneously, because TiO_x is no longer stable in Fe–0.028 mass% Ti at 1473 K but Fe–Ti–O oxide is.

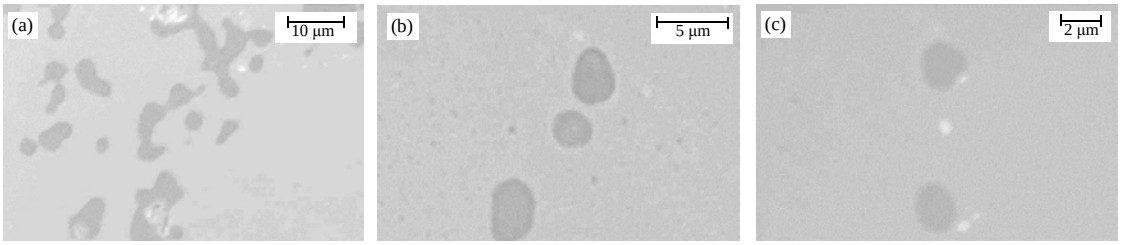

Figure 11 SEM images of typical inclusion observed in Specimen 2–B; (a) as cast, (b) after 60 min heating at 1473 K, and (c) after 180 min heating at 1473 K.

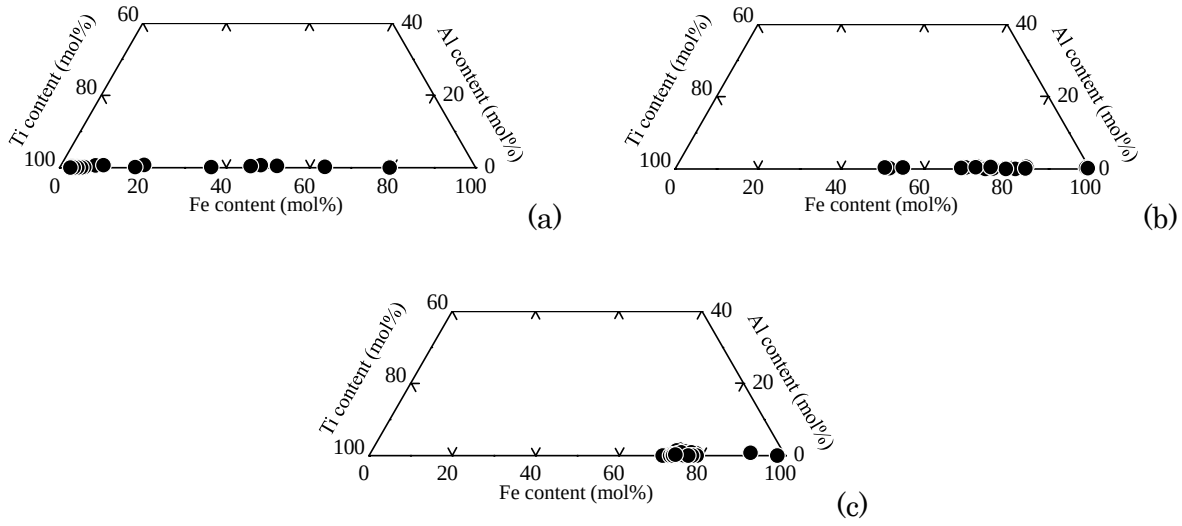

Figure 12 Composition of inclusions in Specimen 2–B; (a) as cast, (b) after 60 min heating at 1473 K, and (c) after 180 min heating at 1473 K.

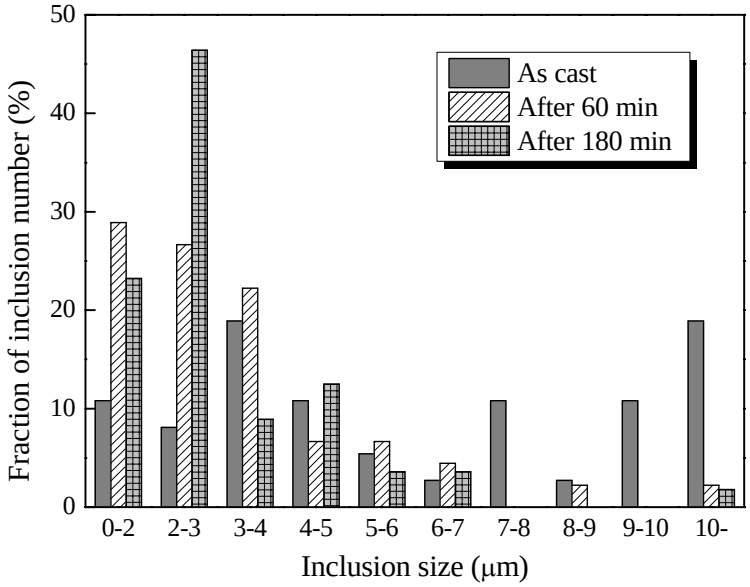

Figure 13　Size distribution of inclusions in Specimen 2–B; (a) as cast, (b) after 60 min heating at 1473 K, and (c) after 180 min heating at 1473 K.

(3) Specimen 2–C (Al: 0.0162 mass%, Ti: 0.29 mass%)

Typical inclusions in as-cast and heated samples of Specimen 2–C are shown in **Fig. 14**. The shape of inclusions in an as-cast sample were similar to those of Specimen 2–B, namely very irregular shape. Although the shape of inclusions did not clearly change by heating at 1473 K, many inclusions in the sample heated for 180 min at 1473 K had two phases in an inclusion as shown in Fig. 14(c)

Figure 15 shows the compositions of inclusions in Specimen 2–C on the Al–Fe–Ti ternary system. Though Al_2O_3 inclusions were mostly observed, various types of inclusions such as TiO_x with small FeO content, or FeO with small Al_2O_3 and TiO_x contents were also found. This is because the metal composition is at the boundary between Al_2O_3, Al_2TiO_5, Ti_2O_3 and Ti_3O_5 stable regions at 1873 K as shown in Fig. 2. Therefore, the formed inclusions have not been equilibrated comprehensively with metal before solidification.

As explained above, the compositions of inclusions changed to two compositions, one is Al–Fe–O inclusions containing approximately 40 mol% Fe as the Al–Fe binary system and also with small Ti content, the other is Al–Ti–Fe–O inclusions which average composition is 20 mol%Al–20 mol%Ti–60 mol%Fe as the Al–Ti–Fe ternary system. Though some Al_2O_3 inclusions were also observed, the fraction of Al_2O_3 inclusions decreased by heating. The changing behavior of inclusion compositions with heating was similar to that observed in the case of Specimen 2–A. However, many observed inclusions in Specimen 2–C after heating had two phases as shown in Fig. 14, which was different

from the case of Specimen 2–A.

Figure 16 shows the size distribution of inclusions. The effect of heating on the change of inclusion size distribution was not clearly observed, which was similar to Specimen 2–A.

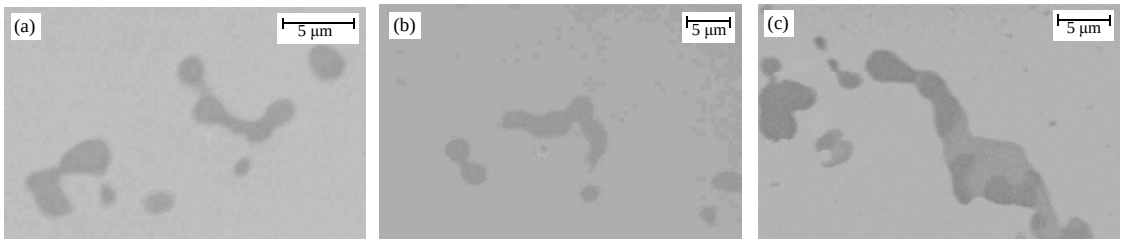

Figure 14　SEM images of typical inclusion observed in Specimen 2–C; (a) as cast, (b) after 60 min heating at 1473 K, and (c) after 180 min heating at 1473 K.

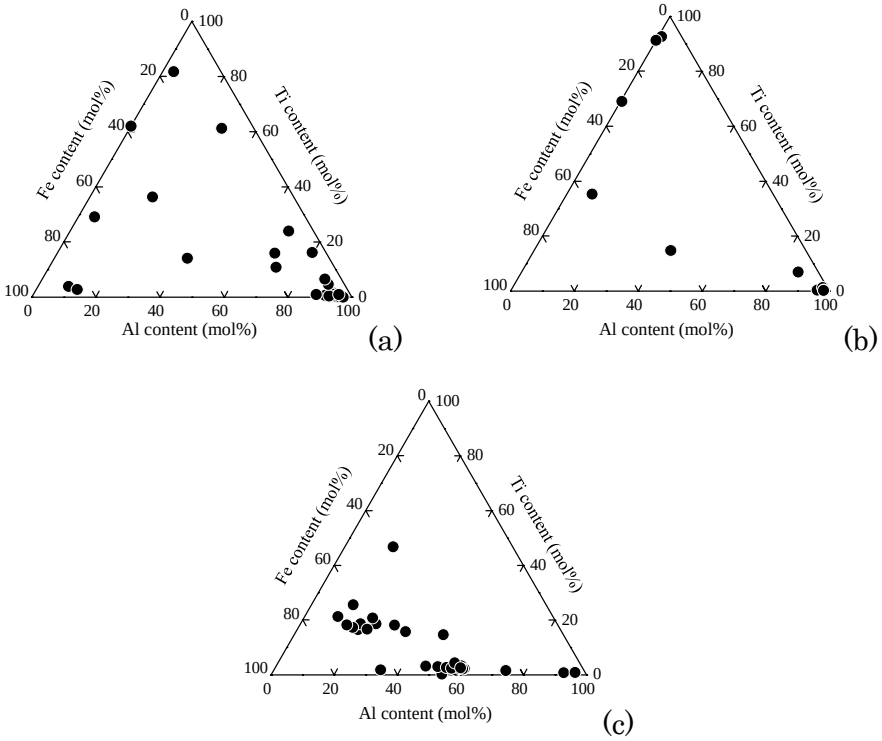

Figure 15　Composition of inclusions in Specimen 2–C; (a) as cast, (b) after 60 min heating at 1473 K, and (c) after 180 min heating at 1473 K.

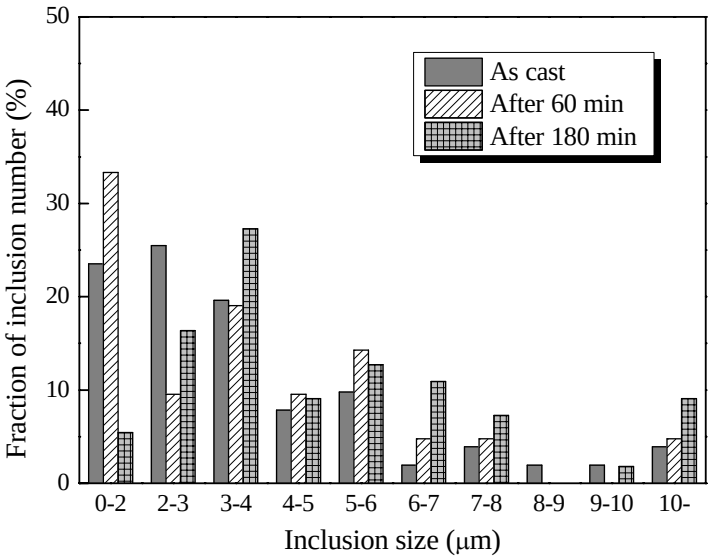

Figure 16　Size distribution of inclusions in Specimen 2–C; (a) as cast, (b) after 60 min heating at 1473 K, and (c) after 180 min heating at 1473 K.

(4) Mechanisms of Size and Compositional Change of Inclusions in Solid State Steels

Effect of heating at 1473 K on the size distribution and composition of inclusion was studied for three different specimens. Regarding the effect on the size distribution, the fraction of smaller inclusions increased in the case of Specimen 2–B, while the size distribution did not change obviously in Specimens 2–A and 2–C. Therefore, the nucleation and dissolution of inclusions expressed as Eqs. (5) and (6) occurred simultaneously and thus the fraction of finer inclusions increased by heating in Specimen 2–B,

$$TiO_x\,(s) \rightarrow \underline{Ti} + x\,\underline{O} \tag{5}$$

$$Fe + \underline{Ti} + (x{+}1)\,\underline{O} \rightarrow FeO\text{–}TiO_x\,(s) \tag{6}$$

On the other hand, the dissolution of inclusions did not occur and therefore the size distribution did not change obviously in the case of Specimens 2–A and 2–C. Although the reason of this difference is not clear at this moment, one possibility is the kinetic effect, namely the dissolution of Al_2O_3 might be much smaller than that of TiO_x.

In the present study, neither the valence of Ti nor the mineralogical phase of inclusions was measured, and the chemical stability of oxide phase in solid steel has not been reported. Therefore, the stability of titanium oxide was evaluated by assuming the condition that Gibbs free energy change for reaction (7) can be applied for solid iron.

$$5\ Ti_2O_3\,(s) = 3\ Ti_3O_5\,(s) + \underline{Ti}\ (\text{mass\%}) \qquad \Delta G^\circ = 189500 - 93.6\,T\ \text{J/mol} \tag{7}$$

As the activity of titanium relative to that in Fe–1 mass%Ti calculated at equilibrium was 0.0148, the titanium oxide in Specimen 2–B is considered to be Ti_2O_3. Furthermore, Fe content in inclusions may be overestimated because of the X-ray signal from Fe matrix during inclusion analysis by EDS as previously explained. From above reasons, the actual average compositions of inclusions in Specimen 2–B would be approximately 30 mol%Ti–70 mol%Fe. When Ti_2O_3 was assumed to be formed as Ti oxide in the sample, the estimated composition of the Fe–Ti–O inclusion corresponds to $4FeO{\cdot}Ti_2O_3$.

The change of inclusion compositions and the final compositions after heating for 180 min at 1473 K were the same for Specimens 2–A and 2–C, namely Al–Fe–O or Al–Ti–Fe–O inclusions. Inclusions firstly changed from Al_2O_3 to Al–Fe–O, and secondly from Al–Fe–O to Al–Ti–Fe–O by heating. Assuming the formation of Ti_2O_3 as a stable titanium oxide and the overestimation of Fe composition as well, the Al–Fe–O (average composition: 60 mol%Al–40 mol%Fe as the Al–Fe binary system) and the Al–Ti–Fe–O (average composition: 15 mol%Al–15 mol%Ti–70 mol%Fe as the Al–Ti–Fe ternary system) inclusions correspond to $Al_2O_3{\cdot}FeO$ and $Al_2O_3{\cdot}Ti_2O_3{\cdot}4FeO$, respectively. However, since these oxide forms were considered based on aforementioned assumptions and no mineralogical phase for this oxide has been reported, further study is required to reveal the form of oxides.

Homogeneous oxide phase in each inclusion was observed in Specimen 2–A, while many inclusions having two phases in one oxide particle were observed in Specimen 2–C. This difference in inclusion morphology between Specimens 2–A and 2–C is not clearly understood and the further study must be conducted.

Since the clear change of size distribution of inclusions by heating was not observed in Specimens 2–A and 2–C, it is considered the dissolution of Al_2O_3 inclusions into Fe matrix did not occur as described previously. Therefore, the change of Al_2O_3 inclusion to Al–Fe–O inclusion, and further change of Al–Fe–O inclusion to Al–Ti–Fe–O inclusion are expressed as Eqs. (8) and (9), respectively.

$$Al_2O_3\,(s) + Fe + \underline{O} \rightarrow Al_2O_3{\cdot}FeO\,(s)$$

or

$$4/3\,Al_2O_3\,(s) + Fe \rightarrow Al_2O_3{\cdot}FeO\,(s) + 2/3\,\underline{Al} \qquad (8)$$

$$Al_2O_3{\cdot}FeO\,(s) + 3\,Fe + 2\,\underline{Ti} + 6\,\underline{O} \rightarrow Al_2O_3{\cdot}Ti_2O_3{\cdot}4FeO\,(s)$$

or

$$5/2\,Al_2O_3{\cdot}FeO\,(s) + 3/2\,Fe + 2\,\underline{Ti} \rightarrow Al_2O_3{\cdot}Ti_2O_3{\cdot}4FeO\,(s) + 3\,\underline{Al} \qquad (9)$$

The oxygen source would be the dissolved oxygen in Fe matrix or the partial dissolution of Al_2O_3, depending on the steel composition. Further physicochemical properties must be clarified for understanding the behavior of inclusions more in detail, such as the chemical

stability diagram for the Fe–Al–Ti–O system in solid steel, or the activities of Al, Ti and O.

4. Conclusions

Equilibrium experiments between molten Fe–Al–Ti metals and Al_2TiO_5 pellets were conducted to determine the important oxide stability diagram for estimation of the phase of oxides produced by Al–Ti deoxidation. However, Al_2TiO_5 phase was not observed at the interface between metal–oxide after equilibrium, but Al_2O_3 phase containing TiO_x and TiO_x phase containing Al_2O_3 were identified. Observation and analyses of non-metallic inclusions in metals after experiments found similar compositions. Therefore, it was concluded that inclusion compositions cannot be estimated from the oxide phase stability diagram determined by the present study and thus further study for the stable oxide phase of the Al_2O_3–TiO_x system is required.

Behavior of non-metallic inclusions in Al–Ti deoxidized steels at 1473 K was studied with three different steels. In the case of Fe–0.0341mass%Al–0.0444mass%Ti and Fe–0.0162mass%Al–0.29mass%Ti, different inclusions were observed in as-cast specimens, while Al–Fe–O and Al–Ti–Fe–O inclusions were observed in both samples after heating at 1473 K and those compositions between two specimens were the same. The size distribution of inclusions did not clearly change by heating. In the case of Fe–0.028mass%Ti, Ti–O inclusions with small content of Fe were observed in an as-cast sample and composition of inclusions changed to Ti–Fe–O after heating at 1473 K, and the fraction of fine and coarse inclusions increased and decreased, respectively. Though the stable phase of oxide equilibrated with Fe–Al–Ti steel at 1473 K has not been clarified, equilibrium phases in solid steel at 1473 K may be different from those at steelmaking temperature and thus the inclusion size distribution, morphology, or composition would change inside solid steel by heat treatment.

Acknowledgment

This research was supported by JFE 21st Century Foundation for FY 2010. The author expresses his great gratitude to their support.

References

1) F. Ruby-Meyer, J. Lehmann and H. Gaye: *Scand. J. Metall.*, **29** (2000), 206.
2) H. Gaye and J. Welfringer: Proc. 2nd Int. Symp. Metall. Slags and Fluxes, Metall. Soc. AIME, Warrendale, PA, USA, (1984), 357.
3) I. Jung, S. A. Decterov and A. D. Pelton: *ISIJ Int.*, **44** (2004), 527.
4) I. Jung, G. Eriksson, P. Wu and A. D. Pelton: *ISIJ Int.*, **49** (2009), 1290.
5) W.-Y. Kim, J.-O. Jo, C.-O. Lee, D.-S. Kim and J.-J. Pak: *ISIJ Int.*, **48** (2008), 17.
6) W. Choi, H. Matsuura and F. Tsukihashi: *ISIJ Int.*, **51** (2011), 1951.

7) H. Itoh, M. Hino and S. Ban-ya: *Tetsu-to-Hagané*, **83** (1997), 773.
8) W.-Y. Cha, T. Miki, Y. Sasaki and M. Hino: *ISIJ Int.*, **48** (2008), 729.
9) Y. Guo and C. Wang: *Metall. Mater. Trans. B*, **21B** (1990), 543.